# Climate drives variability and joint variability of global crop yields

Ehsan Najafi[1,2], Indrani Pal[2,3], Reza Khanbilvardi[1,2]

[1]Civil Engineering Department, The City College of New York, The City University of New York, New York City, USA, 10031

[2]NOAA Center for Earth System Sciences and Remote Sensing Technologies (NOAA-CREST), The City College of New York, The City University of New York, New York City, USA, 10031

[3]Columbia Water Center, Columbia University, New York City, USA, 10025

Corresponding author: Ehsan Najafi, enajafi@ccny.cuny.edu

**Key Points:**

- Decomposing global yield anomalies of four staple crops
- Investigating the most important modes of crop yield variability and their association with large- and local-scale climate
- Identifying co-varying countries and joint dependencies between crop yields

**Abstract**

In this study, long-term national-based yields of maize, rice, sorghum and soybean (MRSS) from 1961 to 2013 are decomposed using Robust Principal Component Analysis (RPCA). After removing outliers, the first three principal components (PC) of the persistent yield anomalies are scrutinized to assess their association with climate and to identify co-varying countries and crops. Sea surface temperature anomalies (SSTa), atmospheric and oceanic indices, air temperature anomalies (ATa) and Palmer Drought Severity Index (PDSI) are used to study the association between the PCs and climate. Results show that large-scale climate, especially El Niño-Southern Oscillation (ENSO) and North Atlantic Oscillation (NAO) are strongly correlated with crop yield variability. Extensive maize harvesting regions in Europe, rice and soybean in South America and sorghum in North America experienced the influence of local climate variability in this period. Sorghum yield variability across the globe exhibits significant correlations with many atmospheric and oceanic indices. Results indicate that not only do the same crops in many countries co-vary significantly, but different crops, in particular maize, in different PCs also co-vary with other crops. Identifying the association between climate and crop yield variability and recognizing similar and dissimilar countries in terms of yield fluctuations can be informative for the identified nations with regard to the periodic and predictable nature of many large-scale climatic patterns.

**Key words:** *Crop yields, Climate, Food security, Joint variability, RPCA*

## 1. Introduction

Numerous studies suggest that weather impacts crop yield variability (*Ray et al.*, 2015; *Chen et al.*, 2004; *Osborne and Wheeler*, 2013). An understanding of the past global climate and crop trends and their linkage provides the opportunity to determine recent yield progress more precisely and project the impacts of climate changes on food availability

(*Lobell et al.*, 2011; *Ray et al.*, 2015). In this regard many studies have been conducted at the local-scale (see more details in *Najafi et al.* (2018a)). Some global studies investigated the links between crop yields and local climate such as precipitation and temperature (*Ray et al.*, 2015; *Osborne and Wheeler*, 2013; *Lobell et al.*, 2011; *Lobell and Field*, 2007) and drought (*Li et al.*, 2009) and a few of them focused on the connection between crops and large-scale climate such as El Niño-Southern Oscillation (ENSO) (*Iizumi et al.*, 2014a; *Abdolrahimi*, 2016), NAO and Indian Ocean Dipole (IOD) (*Heino et al.*, 2018). *Najafi et al.* (2018a) presented a global analysis of the changes in crop yields and their relationship to both large-scale and local climate using a Bayesian multilevel model. It should be noted that separating the influence of climate on crops from other variables is very complicated due to high spatial and inter-annual variability of yields across countries. In this regard, reducing the size of data can help to better understand and interpret its structure, while minimizing information loss.

In a world where about 85% of countries do not have complete food self-sufficiency (*Puma et al.*, 2015), the import of food has enabled many countries to face food security problems by importing crops from other countries (*Porkka et al.*, 2013). But if the influence of climate prompts countries to reduce or suspend crops export, as Argentina, Ukraine, Russia, and Serbia did in the world food crisis during 2007 and 2008, countries that are largely dependent on crops import could face crisis. Export bans in main crop producers would put about 200 million people at risk of hunger (*d Amour et al.*, 2016). Countries that import crops for feeding their population put their people at risk when they depend on a few exporters. One approach to tackling this problem is identifying the countries with similar and dissimilar yield patterns since these countries may be able to trade the excess of their crops during times of food scarcity. Additionally, it is of great importance to recognize the climatic variables that drive these synergistic variabilities across countries. So far, no

efforts have been made to identify whether co-occurrence of yield deficits/surpluses is systematic across the globe.

In this study we used a machine learning approach called Robust Principal Component Analysis (RPCA) to decompose yield time series of maize, rice, sorghum and soybean (MRSS) from 1961 to 2013 to several modes or principal components (PC) to assess the association between crop yields and climate more accurately. Moreover, we use these modes to identify co-varying crop producers and joint dependencies between crops. This paper is organized as follows: section 2 provides the detailed information about the database. Section 3 and 4 presents the methodology and discussion regarding removing outliers and extracting persistent yield anomalies. In Section 5, we present the relationship between the main PCs and local climate and co-varying countries. In section 6, the association between major PCs and large-scale climate will be presented. In section 7, joint dependencies between crop yield variability is discussed. Finally, concluding remarks and highlights will be presented in Section 8.

## 2. Dataset

In this section, we explain different climatic and non-climatic variables, their importance and preprocessing steps.

### 2.1. Crop yields data and standardization methodology

Annual crop yields data from 1961 to 2013 are collected from the Food and Agriculture Organization of the United Nations statistical databases (*FAO*, 2016). In this study, we focused on the countries that have complete yield data in this period. Yields data are standardized using a seven-year moving window (*Troy et al.*, 2015).

$$Y_t = \frac{y_t - \overline{y_{t-3,t+3}}}{std\,(t_{t-3,t+3})}$$ Equation 1

In Equation 1, $Y_t$ is the detrended yield value, $y_t$ is the original yield value, $\overline{y_{t-3,t+3}}$ is the mean of the original yield values for the seven-year moving window, and std($y_{t-3,t+3}$) is the standard deviation of the original yield values for the seven-year window. The detrending approach that is used here leads to losing the first and last three years, So the final time span of detrended yield values are from 1964-2010.

### 2.2. Palmer drought severity index

Palmer drought severity index (PDSI) not only integrates precipitation and temperature, but it is also highly correlated with soil moisture content (*Dai et al.*, 2004a). PDSI ranges from about -10 (dry) to +10 (wet) and represents both dryness or wetness (depending on the region that may imply floods or moderate rainfall (*Dai et al.*, 2004b)). Gridded monthly self-calibrated PDSI, at 2.5-degree resolution, was obtained from NOAA/OAR/ESRL PSD, Boulder, Colorado, USA, from their web site (*NOAA-ESRL*, 2017). Unlike the detrended yields data that are from 1964 to 2010, the time span of PDSI (and other climatic variables) is from 1963 to 2010, since the association between PCs and PDSI (and other climatic variables) with one-year lag will be considered in this study.

### 2.3. Air temperature anomalies (ATa)

Monthly temperature anomalies data of the University of Delaware Air Temperature & Precipitation, at 0.5-degree resolution provided by the NOAA/OAR/ESRL PSD, Boulder, Colorado, USA, from their web site (*NOAA-ESRL*, 2017).

### 2.4. Sea Surface temperature anomalies (SSTa)

Monthly Extended Reconstructed Sea Surface Temperature (ERSST) version 4 dataset, at 2.5-degree resolution, provided by the NOAA/OAR/ESRL PSD, Boulder, Colorado, USA, from their web site (*NOAA-ESRL*, 2017).

## 2.5. Oceanic and atmospheric indices

Multiple monthly atmospheric and ocean time series (*NOAA-ESRL*, 2017) are used to study the links between large-scale climatic patterns and modes of crop yield variability. The detailed information of these indices are provided in Table 1.

**Table 1.** Oceanic and atmospheric indices discussed in this study

| Name of index (abbreviation) | Description | Reference |
|---|---|---|
| Eastern Tropical Pacific SST (Nino 3) | SST in Tropical Pacific measured at 5N-5S and150W-90W. | |
| Central Tropical Pacific SST (Nino 4) | SST in Tropical Pacific measured at 5N-5S and 160E-150W. | |
| East Central Tropical Pacific SST (Nino 3.4) | SST in Tropical Pacific measured at 5N-5S and 170W-120W. | |
| Extreme Eastern Tropical Pacific SST (Nino 1+2) | SST in Tropical Pacific measured at 0-10S and 90W-80W. | |
| Multivariate ENSO index (MEI) | The first seasonally varying principal component of six atmosphere-ocean variable fields in the Tropical Pacific basin. | *Wolter and Timlin* (2011) |
| Oceanic Nino Index (ONI) | Three months running mean SST anomalies in the Nino 3.4 region, based on changing base period. | *Trenberth and Stepaniak* (2001) |
| Pacific Decadal Oscillation (PDO) | The first PC of monthly SST anomalies in the North Pacific Ocean. | *Mantua and Hare* (2002) |
| Tripole Index for the Interdecadal Pacific Oscillation (TPI-IPO) | The difference between the SSTa averaged over the central equatorial Pacific and the average of the SSTa in the Northwest and Southwest Pacific. | *Henley et al.* (2015) |
| North Pacific Pattern (NP) | Area-weighted sea level pressure over 30N-65N and 160E-140W. | *Trenberth and Hurrell (1994)* |
| Pacific/ North American pattern (PNA) | Geopotential height anomalies (usually at 700 or 500 hPa) observed over the eastern and western US. | *Leathers et al. (1991)* |
| West Pacific Index (WP) | A primary mode of low-frequency variability over the North Pacific. | *Wallace and Gutzler (1981)* |
| Caribbean SST Index (CAR) | The time series of SSTa averaged over the Caribbean. | *Penland and Matrosova (1998)* |
| East Atlantic Pattern (EAP) | The second prominent mode of low-frequency variability over the North Atlantic. | |
| North Atlantic Oscillation (NAO) | Surface pressure dipole between Iceland and the Azores. | *Leathers et al. (1991)* |
| Tropical Southern Atlantic (TSA) | Anomaly of the average of the monthly SSTa at 0-20S and 10E-30W | *Enfield et al. (1999)* |
| Atlantic Multidecadal Oscillation (AMO (unsmoothed)) | Average SSTa in the North Atlantic Ocean over 0-80N to measure the variability occurring in the North Atlantic Ocean. | Enfield et al. (2001); Kerr (2000) |
| Western Hemisphere warm pool (WHWP) | Monthly anomaly of the ocean surface area warmer than 28.5 degree Celsius in the Atlantic and eastern North Pacific and eastern North Pacific | Wang and Enfield (2003a). |
| Quasi-Biennial Oscillation (QBO) | A quasi-periodic oscillation of the equatorial zonal wind between easterlies and westerlies in the tropical stratosphere. | Baldwin et al. (2001) |
| Southern Annular Mode (SAM) | Pressure dipole between the Antarctic and Southern and Hemisphere mid latitudes. | Marshall (2003) |

## 2.6. Global coverage of MRSS croplands

In order to obtain the global spatial coverage of MRSS croplands, we combined the irrigated and rain fed maps for each crop (*Portmann et al.*, 2010; *ORNL*, 2016). The resulting maps are used to specify the spatial coverage of croplands as well as croplands areas (in hectare (ha)) in the countries of this study that are impacted by local climate variability.

## 3. Methodology

Principal component analysis (PCA) is one of the most widely used statistical methods for dimensionality reduction. However, its drawback regarding the treatment of outliers may put its validity in question (*Candes et al.*, 2009). Basic statistical methods often result in unreliable results in the presence of outliers (*Demsar et al.*, 2013). This prompted us to use the robust version of PCA. In this study we employed RPCA as a machine learning approach. RPCA decomposes a rectangular matrix M into a low-rank component (L matrix), and a sparse component (S matrix), by solving a convex program called Principal Component Pursuit (*Candes et al.*, 2009).

$$min(||L||_* + \lambda||S||_1) \quad \text{Equation (2)}$$

$$L + S = M \quad \text{Equation (3)}$$

$||L||_*$ is the nuclear norm of L. In Equation 2 lambda is the parameter of the convex problem that is minimized in the Principal Components Pursuit algorithm (*Candes et al.*, 2009). RPCA computes the S matrix in a way that minimizes the norms, so RPCA yields lower number of PCs than ordinary PCA. In our case, M represent the yield anomalies matrix. One dimension of M is time (1964 to 2010) and other dimension is countries (location) and the values are locally (country-wise) detrended yield anomalies. The S matrix contains all the simultaneous anomalous values and the L matrix exhibits detrended yields without outliers in the countries from 1964 to 2010. The values in the S matrix may be considered poor observations due to biased measures or true values, so the S matrix should be carefully evaluated to see if the values are errors or valid numbers. Exploring the S matrix is not in the scope of this study and demands a separate investigation. In this study, the L matrix will be scrutinized in detail.

## 4. Low rank matrix; persistent yield anomalies

Crop yields anomalies in some years to a great extent are positively or negatively larger than other years. These anomalies may be attributed to unusual favorable or extreme climatic patterns. Lots of the values in the S matrix are zero since large positive or negative yield spikes do not happen frequently across the global countries. L matrix that contains persistent yield anomalies, delivers three types of results: loadings, eigenvalues and scores. Loadings that contain uncorrelated PCs are linear combinations of the actual variables (*Jolliffe*, 2002).

Each PC that is constructed from the L matrix, explains part of global yield variability. Here, RPCA decomposed the yield anomalies of MRSS into 28, 28, 27 and 20 components respectively. The first PCs contain the maximum variation of the original variables and vice versa. Eigenvalues provide a measure of the variance explained by each PC. In this study, the first 3 PCs are retained for detailed analysis. These PCs of MRSS explain 24%-31% of the total yields variance of the L matrix. Each PC is associated with a score vector. Scores are normalized yield time series and can be used to find links between PCs with other variables (such as climatic time series) by means of correlation analysis. It should be noted that the time-span of MRSS yield anomalies is from 1964 to 2010, so the score vector of each PC refers to this period. In each PC, countries with positive values have a direct relationship with that PC (and vice versa) and the magnitude defines the power of this association. So, in each PC, the countries with a large loading value are of significant importance. These countries not only co-vary similarly/oppositely (same loading sign value countries co-vary similarly and vice versa), but they explain the variance of that PC the most. Hence, large loading value countries (LLVC) will be explored in further detail. The distribution of the loadings values of the first three PCs (Figure 1) show that normal density, with a good approximation, fits loadings values.

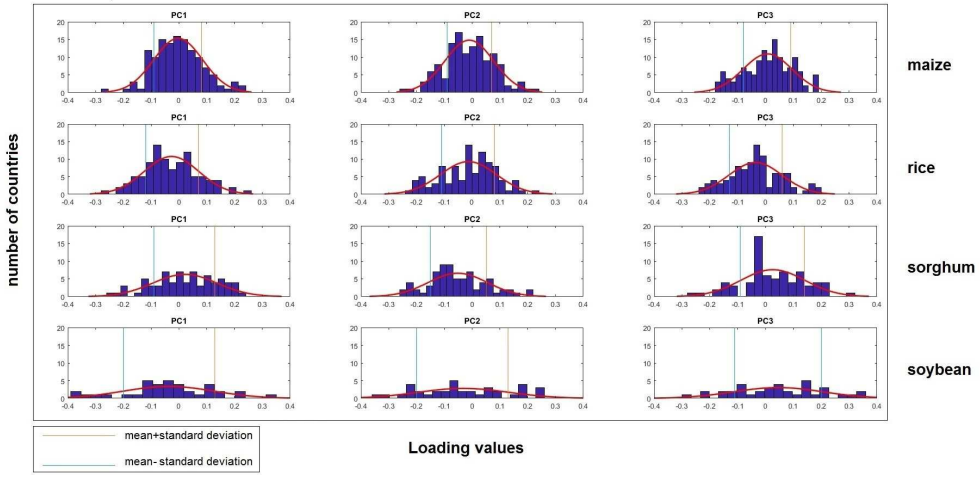


**Figure 1.** The histogram of the loadings of the first 3 PCs acquired from the L matrix and a fitted normal density curve. The vertical blue (orange) lines show mean minus (plus) one standard deviation for the loadings values for each PC.

Therefore, we choose the LLVC based on one standard deviation exceedance of loadings values from the mean from both sides in each PC. Figure 2 depicts the countries that have large loadings values in many PCs (at least 12, 11, 8 and 10 times across all PCs of MRSS respectively). These countries explain a large part of variability in the corresponding PCs and yield anomalies in these countries are more volatile than other countries. Among the identified countries in Figure 2, Brazil and Peru (sorghum, soybean), South Korea (maize, sorghum, soybean), Argentina (soybean), Bolivia (rice), Gambia and Sri Lanka (maize, sorghum) have many large loading values across PCs for more than one crop. Four out of seven of these countries are located in South America. There is considerably large variability of soybean in North and South America and Middle and Southern African countries. Most of the identified sorghum producing countries are located in the mid latitude.

Here, spearman correlation is used to assess the association between climate and PCs in both concurrent and one-year lag phases. It should be noted that correlation does not

show out-of-sample predictive power (Friedman and Schwartz, 1991) or causation. We only report

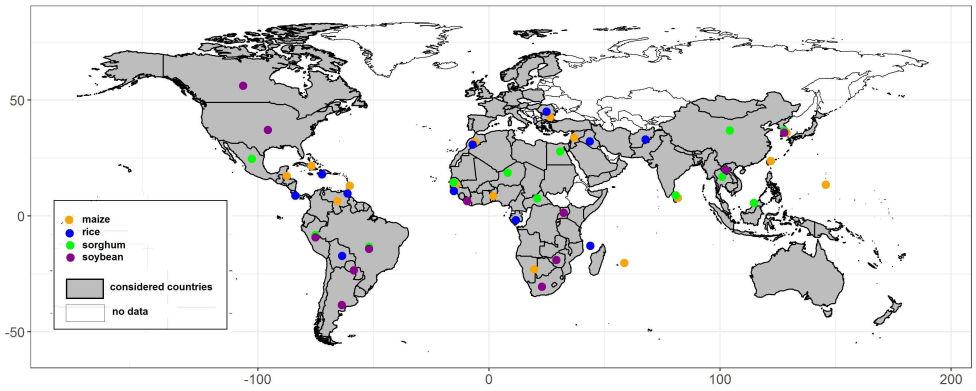


**Figure 2.** The countries with large loadings values in at least 12, 12, 11, 8 and 10 PCs (40% of PCs) acquired from L matrix of MRSS respectively.

the correlations with significance level lower than 0.05. However, the first few PCs easily interpreted in many climatological and meteorological examples (*Jolliffe*, 2002), they are not always associated with meaningful physical phenomena and are not always easy to interpret (*Demsar et al.*, 2013). Figure 3 (Figure 4) presents concurrent correlation (CC) and one yearlag correlation (LC) between the first three PCs of MRSS and annual average of SSTa and ATa (PDSI). In both Figure 3 and Figure 4 we showed significant correlations (95%) with SSTa. Significant correlations over croplands of MRSS are marked with small black dots.

The boundary of LLVC are highlighted in orange (large positive loading values) and blue (large negative loadings values). Throughout the manuscript, all the reported numbers are based on the countries that are considered in this study. For example, global maize production/cropland area refers to production/cropland area of maize in 130 countries of this study.

## 5. Climate variability across MRSS croplands and co-varying nations

LLVC in PC1-PC2-PC3 account for 16%-14%-13%, 4%-8%-10%, 52%-32%-49%, 72%-41%-35% of the global MRSS production. As it can be seen a great deal of global yields variability of sorghum and soybean anomalies happen in a limited number of co-

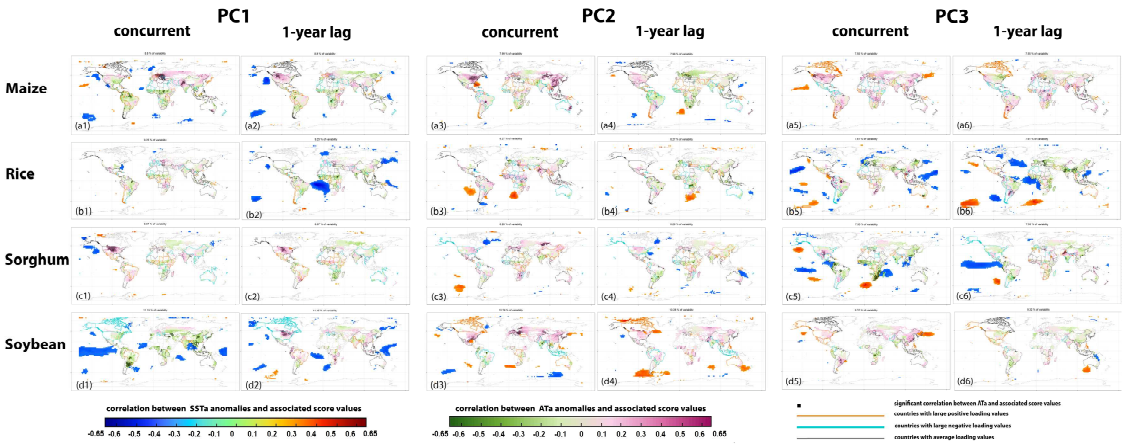


**Figure 3.** Concurrent (one-year lag) correlation between the PC1, PC2 and PC3 of maize, rice, sorghum and soybean and SSTa and ATa over croplands from 1964 to 2010 (1963-2009). These three PCs explain about 24%, 25%, 25%, 31% of the global maize, rice, sorghum and soybean yield variabilities in the low rank matrix respectively from 1964 to 2010. The locations with statistically significant correlations (95%) over croplands are designated with small black dots and only significant correlation (95%) between SSTa and the score of each PC are depicted. The boundary of the countries with large positive (negative) loading values are highlighted in orange (blue).

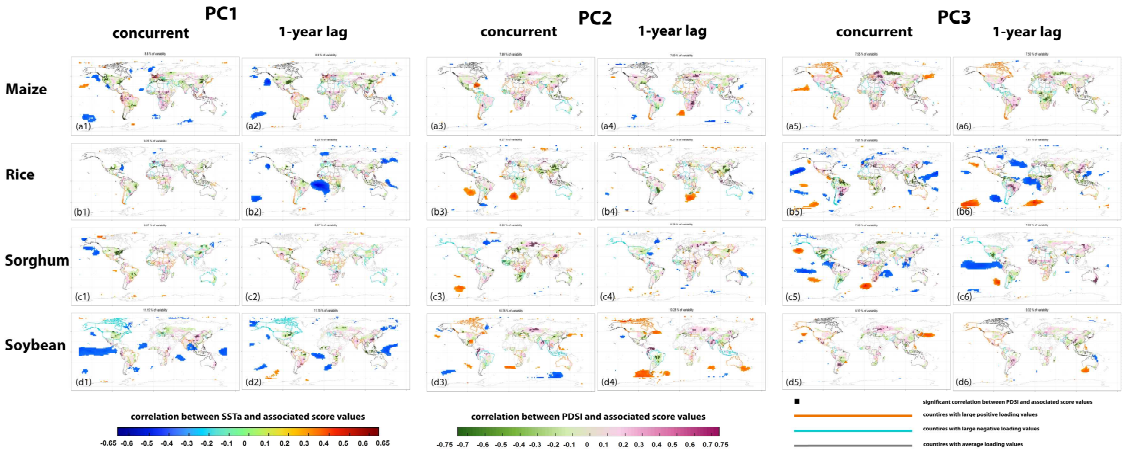


**Figure 4.** Concurrent (one-year lag) correlation between PC1, PC2 and PC3 of maize, rice, sorghum and soybean and SSTa and PDSI over croplands from 1964 to 2010 (1963-2009). See the caption of Figure 3 for more details.

varying countries with large production. Here, we computed the area of some regions that are impacted by AT or PDSI, in either concurrent or lag phase (from now on we call it the regions that are impacted by local climate). Globally, in PC1-PC2-PC3, 21%-26%-10% of maize harvesting regions, 6%-30%-23% of rice croplands, 8%-6%-16% of sorghum harvesting regions, and 46%-17%-15% of soybean harvesting regions of major producer countries were influenced by local climate. Many of these croplands are located within LLVC. In this study, major producers (MP) are the first 20 maize, rice, sorghum and soybean producers in 2013 based on the countries of this study (see Table S2-a for more information).

In total, PC2-rice (45 million hectare (mha)), PC2-maize (38 mha) and PC3-rice (36 mha) represent the largest impacted croplands by local climate. Table 2 presents the percentages of croplands with significant local climate variability (SLC). PC2-maize (25 mha), PC1-soybean (13 mha), PC2-rice (18 mha) and again PC2-rice (24 mha) exhibit the largest percentages of impacted croplands by AT, AT-lag, PDSI and PDSI-lag respectively. On average, SLC in sorghum croplands is smaller than the other three crops. 41 maize producers (most of them are located in Africa, Central America and Southeast Asia), 9 rice producers (Comoros, Belize, Honduras, Jamaica, Nicaragua, Trinidad and Tobago, Sri Lanka, Timor-Leste, Taiwan), 9 sorghum producers (Central African Republic, Guinea-Bissau, Rwanda, Uganda, Dominican Republic, Haiti, Iraq, Lebanon, South Korea) and 3 soybean producers (Liberia, Suriname, Taiwan) did not show any SLC in PC1-PC3. However, many of these countries exhibit SLC in other PCs.

Figure 3 and Figure 4 show that the impact of ATa and PDSI in both concurrent and lag phases vary among countries/regions in different PCs. The ratio of impacted cropland areas by local climate in Figure 3 and Figure 4 for 10 regions (See Table S1 for the countries of each region) are shown in Figure 5. In PC1 56% of maize harvesting regions in Europe, 40% of sorghum harvesting regions in North America and 49% of soybean

harvesting regions in South America experienced the influence of ATa. 30% and 43% of sorghum and soybean harvesting regions in PC1 in North America were impacted by ATa-lag. PDSI and

**Table 2.** The percentages of MRSS croplands that experienced local climate variability in PC1 to PC3

| | AT | | | AT (one-year lag) | | | PDSI | | | PDSI (one-year lag) | | |
|---|---|---|---|---|---|---|---|---|---|---|---|---|
| | PC1 | PC2 | PC3 | PC1 | PC1 | PC2 | PC1 | PC2 | PC3 | PC1 | PC2 | PC3 |
| maize | 7.3 | 19 | 4.1 | 0.3 | 3 | 1.5 | 11 | 3.4 | 2.7 | 12 | 4.7 | 3.9 |
| rice | 0.2 | 1.4 | 6.1 | 0.7 | 2.1 | 6.5 | 2.5 | 13 | 6.5 | 4 | 16 | 8.6 |
| sorghum | 5.2 | 0.9 | 9.9 | 4.2 | 0.9 | 7.9 | 1.3 | 3.6 | 8.1 | 1.7 | 2.6 | 4.8 |
| soybean | 18 | 5.4 | 1.2 | 18 | 0.2 | 0.4 | 4.4 | 1.5 | 11 | 12 | 13 | 2.7 |

PDSI-lag extensively impacted soybean croplands in Oceania (47%) and maize croplands in East Asia (30%). In PC2 CC with ATa is more prominent than AT-lag especially for maize croplands in North America (42%) and soybean in Europe (29%). PDSI-lag was crucial over 47% soybean harvesting regions in South Asia. In PC3, rice and sorghum yield variabilities were impacted by ATa in both phases mostly in rice harvesting regions of Oceania (ATa, 37%), sorghum in West Asia (AT-lag, 49%) and South Asia (AT-lag, 25%). PC3 is indicative of a strong association with PDSI in some regions including rice croplands in South America (PDSI, 39%), sorghum croplands in North America (PDSI, 41%), South America (PDSI,

38%), southeast Asia (PDSI, 46%), Caribbean (PDSI-lag, 45%), and soybean croplands in South America (PDSI, 31%).

Figure 6 demonstrates the croplands area in 10 MP that experienced local climate variability. In this figure, the overlappings of the impacted croplands area by ATa, ATa-lag, PDSI and PDSI-lag are not considered. A large extent of maize harvesting regions in China and US, rice in China, India and Thailand, sorghum in US, Mexico, India and Argentina and soybean in US, Brazil and Argentina experienced the influence of local climate variability.

More than half of Maize croplands in France, Hungary, Romania, South Africa, US and Pakistan, rice in Brazil, Bangladesh, South Korea, sorghum in South Africa, Canada, US, Indonesia

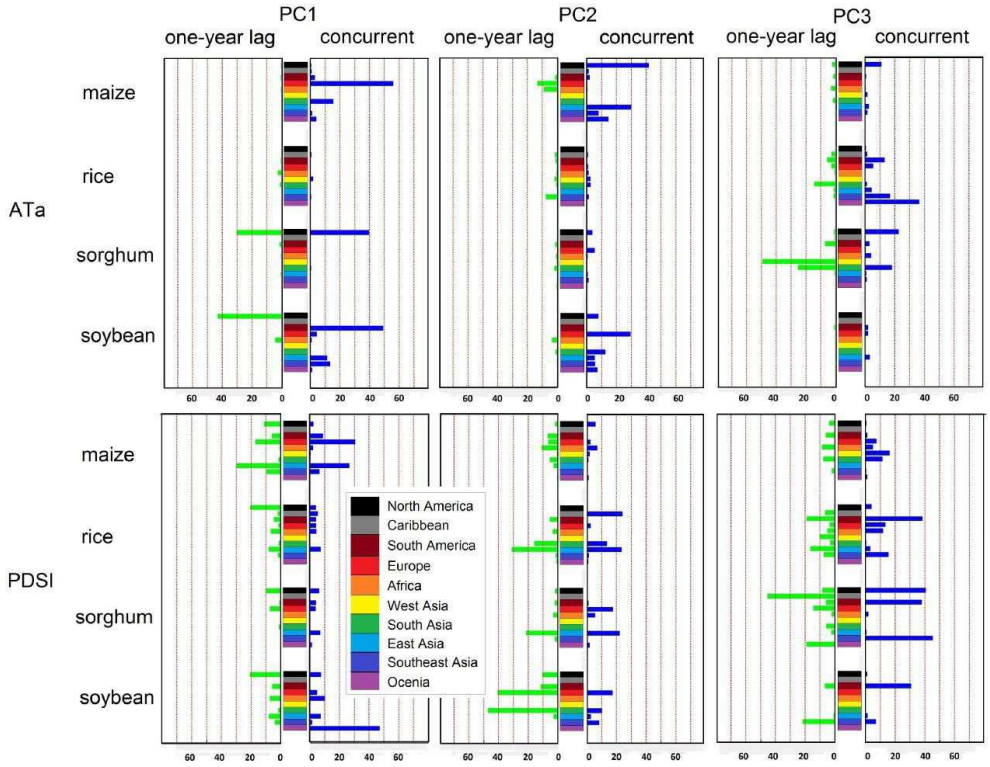


**Figure 5.** The percentages of MRSS croplands in 10 global regions that experienced local climate variability in PC1 to PC3

and Viet Nam and soybean in Italy, Romania, Turkey, Canada, Mexico, US, Argentina, Viet Nam and Japan impacted by local climate in at least one PC.

Crop yield variability in major global crop exporters (ME) is crucial since many of importers, particularly major importers (MI) are dependent to these countries. Among maize producers, Brazil, France, Germany, Poland, Romania, Hungary, Bulgaria, Canada, Argentina (ME) and Morocco, Egypt, Taiwan, Iran, Peru, Venezuela, Chile, Colombia (MI) co-vary conversely in different PCs. Within rice producers, Spain, Paraguay, Romania, Hungary, Bulgaria, Uruguay, Argentina, Cambodia, Australia, Thailand (ME) and Cameroon, Ghana, Venezuela, Iran, Angola, Iraq (MI) are major exporters and major

importers that co-vary in an opposite manner across different PCs. Among sorghum producers, Hungary, Paraguay, Australia, Thailand, US, South Africa (ME) and Papua New Guine, Chad, Kenya, Sudan, Egypt, Colombia, Somalia (MI) and among soybean producers Brazil, Uganda, India, Romania, Canada, US, Indonesia (ME) and South Korea, Taiwan, Colombia and Vietnam (MI) are examples of LLVC that co-vary conversely in different PCs (See Table S2-b,c for the import and export ranks of countries in 2013). However, not all of the identified countries here trade with each other, but free trade between countries not only can be one part of the solution to global food security but it improves sustainable use of natural resources (*Heisey*, 2015).

## 6. PCs' links with large-scale climate

Global drivers of atmospheric variability such as ENSO or NAO influence local climate across the globe (*Steptoe et al.*, 2017; *Pournasiri Poshtiri and Pal*, 2014, *Armal et al.*, 2018) and subsequently can trigger simultaneous impacts on croplands. The relationship between crop yield variations and large-scale climate can be justified if those local climate variables are consequences of large-scale climate variabilities. In this section, we examine significant SSTa (sSSTa) in Figure 3 and the relationship between PCs and indices in Table 1. sSSTa are identified across many geographical locations in the Pacific Ocean (Figure 3c6-d1), Atlantic Ocean (Figure 3-b2-b6), Indian Ocean (Figure 3-d1), etc. Some PCs exhibit

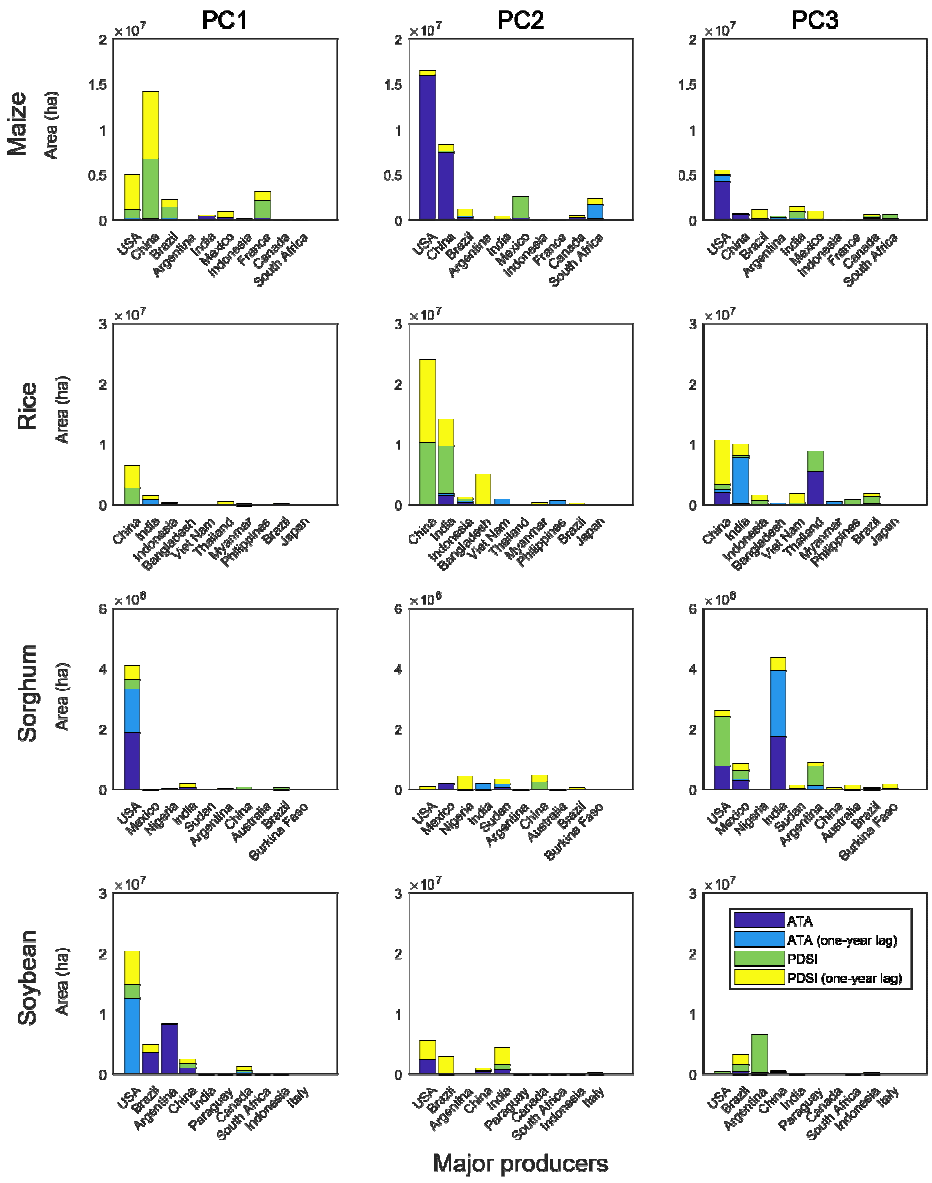


**Figure 6.** Impacted MRSS croplands area by ATa and PDSI in both concurrent and lag phases in 10 major MRSS producers in PC1 to PC3

sSSTa that can be easily connected to well known climatic patterns, such as PC3-sorghum (Figure 3-c6) where sSSTa in the Tropical Pacific Ocean resembles the well known ENSO pattern. Moreover, it is already proved that localized SST variations can impact neighboring croplands (*Shi et al.*, 2015; *Dado and Takahashi*, 2017). Figure 3 and Figure 4 present some cases that may fall in this category. For example, significant ATa (sATa) in

the north of Madagascar, Zimbabwe, South Africa and Mozambique (Figure 3-c5) may be associated with sSSTa around Madagascar. Other example are sSSTa over Sea of Okhotsk and sATa in soybean harvesting regions of Japan (Figure 3-d5) and sSSTa in the Gulf of Mexico and sATa over soybean croplands of US (Figure 3-d3).

Identifying the most impactful SSTa demands correlation analyses with various lead times. So, in Figure 3 (where SSTa features are based on annual average of climatic variables) all sSSTa may not be reflective of impactful patterns. Here, correlation between indices and PCs have been computed considering both annual averages of the indices and the December-January-February (DJF) seasonal average, both in concurrent and lag phases. This may give us more insight into identifying the most prominent oceanic and atmospheric mechanism behind these features. If a PC is largely correlated with both seasonal and annual average of an index, the one with larger correlation will be presented. There are several SST indices to characterize the nature of ENSO which are based on SSTa averaged across a given region in the Pacific Ocean (*Trenberth and Stepaniak*, 2001). These Nino indices, as well as Multivariate ENSO Index (MEI) and Oceanic Nino Index (ONI) are all used to describe ENSO (we call them ENSO indices). Among all the significant correlations with ENSO indices, the index with the largest correlation magnitude will be reported.

ENSO is the major mode of coupled atmosphere-ocean in the Tropical Pacific Ocean. At a first glance to sSSTa (Figure 3), we recognize an extensive sSSTa in the Tropical Pacific Ocean in different PCs that among them the lag map of PC3-sorghum (Figure 3-c6) and concurrent map of PC3-soybean (Figure 3-d1) are more prominent. The patterns in these two cases increase the likelihood of a link between ENSO and climate variability over croplands such as sorghum harvesting regions of US and South Africa and soybean harvesting regions of China and Brazil. All the crops are significantly correlated with at least one of the ENSO indices. PC3-rice, PC3-sorghum and PC1-soybean in both lag and

concurrent phases and PC1-maize in concurrent phase are associated with ENSO. Unlike sorghum and rice, soybean shows different sign correlations with ENSO in concurrent and lag phases (33% and 36%). PC3-sorghum, in both concurrent and lag phases, has the largest correlation magnitude (about -52%) with ENSO indices. PC1-soybean in the lag phase is only correlated with Nino 4. We found the association between PC3-rice (PC3-sorghum) and all of the ENSO indices in concurrent (lag) phase to be significant. ENSO's effect on crop yields was already established in the 1980s (*Handler*, 1984). A plethora of studies have been conducted on the impacts of ENSO on crops such as maize in the US (*Mourtzinis et al.*, 2016; *Legler et al.*, 1999; *Hansen et al.*, 1998), rice in China, Myanmar, Vietnam, US, Australia, North Korea, the Philippines, Central America and Europe (*Chen et al.*, 2008; *Iizumi et al.*, 2014b), sorghum in South America (*Podesta et al.*, 1999), etc.

PC3-rice (concurrent) and PC3-sorghum (lag and concurrent) are associated with Tripole Index for the Interdecadal Pacific Oscillation (TPI-IPO) (*Henley et al.*, 2015). In these two PCs sSSTa can be seen in regions over the Pacific Ocean where TPI-IPO index is computed (Figure 3-b5-c5). CC between PC3-sorghum and seasonal TPI-IPO is the largest correlation magnitude found in this section (-0.55%). The Pacific Decadal Oscillation (PDO) pattern is centered over the mid-latitude Pacific basin (*Mantua and Hare*, 2002). PC2-soybean is well correlated with PDO in the concurrent phase. This climatic pattern impacts temperature in Mexico to the southeast of the US and precipitation in Mexico to the southwest of the US, Canada, Australia and India (*Mantua and Hare*, 2002; *Power et al.*, 1998; *Krishnan and Sugi*, 2003). Mexico, US, Canada and India exhibit climate variability over soybean croplands of PC2-soybean (Figure 3-d3 and Figure 4-d3). This is more prominent in India since this country is among LLVC. Caribbean SST Index (CAR) (*Penland and Matrosova*, 1998) that is based on SSTa over the Caribbean is only correlated with the lag phase of PC1sorghum during DJF. The most important feature of this PC is sATa in the Great Plains of US (Figure 3-c2). The CC between annual average

of North Pacific pattern (NP) (*Trenberth and Hurrell*, 1994) and PC3-sorghum is crucial. It has been reported that NP impacts temperature in west of North America and precipitation over Great Plains (*Linkin and Nigam*, 2008a). We found an extensive climate variability over sorghum harvesting regions of this PC (Figure 3-c5 and Figure 4-c5). West Pacific (WP) influences precipitation over the Pacific northwest and south central of Great Plains (*Linkin and Nigam*, 2008b; *Gershunov and Barnett*, 1998). PC3-sorghum exhibits the largest correlation with annual average of WP (CC). In this case US exhibits a large extent of sPDSI (Figure 4-c5). Pacific/ North American pattern (PNA) index is associated with both temperature and precipitation (*Leathers et al.*, 1991). PNA impacts temperature over the west, south and southeast of US and precipitation in the Pacific Northwestern and upper Midwestern US. *Rogers and Rohli* (1991) have related crop damage in Florida to incidences of PNA and *Garnett et al.* (1998) used PNA to forecast the weather over crop-growing regions in Canada. PC1- and PC3-sorghum are correlated with annual average of PNA (CC) and extensive croplands in North America in these two PCs were found to have a large correlation with ATa (Figure 3-c1-c5) and PDSI (Figure 4-c1-c5). The Western Hemisphere Warm Pool (WHWP) develops in the west of Central America. It appears in spring and is active until early Fall and it is linked with rainfall from northern South America to the southern tier of the US (*Chunzai and B.*; *Wang and Enfield*, 2003b). The CC between PC3-sorghum and annual average of WHWP is 50% (see the sSSTa in and west of Central America in Figure3-c5). Sorghum croplands in Mexico and US present an extensive SLC (Figure 3-c5 and Figure 4-c5). In this case, we computed the average of WHWP index during different months. Results show that the average of WHWP in March to May is highly correlated with PC1-soybean (-40%).

North Atlantic Oscillation (NAO) is more apparent in the winter and is characterized by the NAO index. Here, all the crops in one PC are significantly correlated with NAO. The most prominent one is PC3-rice (-42%). NAO influences crop yields in the US, Europe (*Kim and*

*McCarl*, 2005; *Gimeno et al.*, 2002; *Tian et al.*, 2015; *Gouveia et al.*, 2008), China, southeast of Asia, the Middle East, northeastern Africa, northeast of India and northeast of Australia (*Heino et al.*, 2018; *Guiling and Liangzhi*, 2004). *Guiling and Liangzhi* (2004) found a long delay response of vegetation to the NAO index in Asia. They pointed out that it can be associated with carbon and nutrient cycling and biochemical responses to climate. PC1-rice, PC3-rice and PC3-sorghum are associated with the annual average of Tropical Southern Atlantic Index (TSA) with a one-year lag. PC1-rice and PC3-rice exhibit sSSTa in regions in the Atlantic Ocean where this index is computed (Figure 3-b2-b6). There is evidence of an association between rainfall over Central Equatorial Africa and TSA (*Hirst and Hastenrath*, 1983; *Camberlin et al.*, 2001; *Nicholson and Entekhabi*, 1987). sPDSI can be seen in DR Congo (Figure 4-b2), Sudan, Chad, Nigeria and Central African Republic (Figure 4-b6).

*Gonsamo et al.* showed the global association between NDVI and Atlantic Multidecadal Oscillation (AMO), but its impact on crops has not been explored yet. PC3-rice and seasonal AMO in the lag phase are correlated. Rice harvesting regions in this PC in Brazil, Morocco, Central African countries and east of Europe present sPDSI (Figure 4-b6). It has been reported that rainfall variability in northeast of Brazil, African Sahel and climate of North America and Europe are related to AMO (*Knight et al.*, 2006). Indian Ocean Dipole (IOD) (*Saji et al.*, 1999) impacts rainfall in Pakistan and south of China and temperature and precipitation in Europe, northeast of Asia, North and South America, South Africa, south of Iran and southwest Australia (*Saji and Yamagata*, 2003). IOD's influence on crop productivity in Australia and North America has already been discussed in *Yuan and Yamagata* (2015) and *Heino et al.* (2018). PC2-soybean with IOD was found to be significant in the concurrent phase. Many of the aforementioned countries exhibit local climate variability across soybean croplands (Figure 3-d3 and Figure 4-d3). We found a significant correlation between PC1-soybean and Quasi-Biennial Oscillation (QBO) in

concurrent phase. The impact QBO on corn in the US and South Africa has been investigated (*Malone et al.*, 2009; *Jury*, 2002). Southern Annular Mode (SAM) is the only index that is significantly associated with PC3maize (in concurrent phase) and PC2-soybean (in concurrent and lag phases). SAM has a significant correlation with rainfall in China (*Nan and Li*, 2003), South Africa (*Engelbrecht and Landman*, 2016), South Asia (*Prabhu et al.*, 2017) and southern and eastern Australia (*Steffen et al.*, 2011). sPDSI can be seen in South Africa, Australia (Figure 4-a5) and India (Figure 4-d3-d4). In total, sorghum and maize have the highest and lowest number of significant correlations with the indices studied here, respectively. We did not find any links between PC2-maize, PC2-rice and PC3-soybean and the climatic indices.

## 7. Joint dependencies between MRSS

We tested joint dependencies among MRSS yield anomalies. The spearman correlation between all the combinations of the first 3 PCs of MRSS is computed to assess any association between their variations. Results indicates that PC2-soybean and PC2-sorghum present the largest positive (0.42%), and PC3-rice and PC1-maize present the largest negative (-0.53%) correlations. Sorghum and rice, soybean and rice, and maize and soybean only in one PC are strongly correlated. Maize in different PCs co-varies with sorghum and rice. Figure 7 depicts the scatter plots of the PCs with significant correlation. These results are based on the yield variations in different number of countries. In order to have more coherent results we evaluated joint dependencies of MRSS in Argentina, Australia, Brazil, China, Colombia, DR Congo, India, Italy, Mexico, North Korea, Pakistan, Peru, Romania, South Korea, Tanzania, USA and Zimbabwe that have complete detrended yield data set from 1964 to 2010. These countries account for 76%, 56%, 55% and 89% of global MRSS production. Results show that PC3-rice and PC3-soybean within

these countries present the largest positive (0.37%) and PC2-maize and PC3-soybean present the largest negative (-0.41%) correlations.

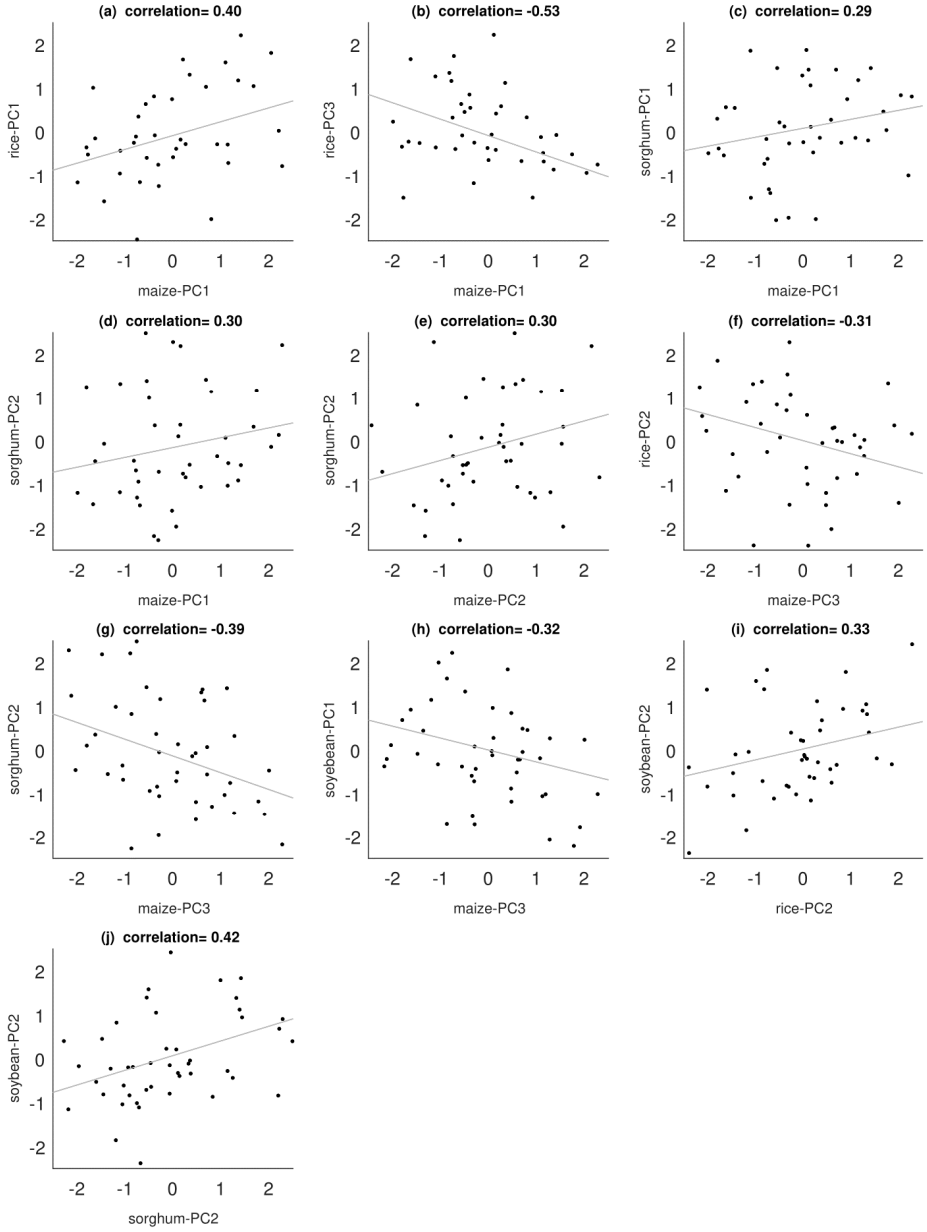


**Figure 7.** Scatter plots between PC1 to PC3 with significant spearman correlation (95% confidence interval)

## 8. Conclusion

The global population is expected to reach 9.7 billion in 2050, climate extremes such as floods and droughts have had an uptrend since the last century in many countries across the globe (*Asadieh et al.*, 2016; 2016; *Poshtiri and Pal*, 2016; *Najafi et al.*, 2018b; *Armal and Al-Suhili*, 2019) and changing diets and demand

for meat and dairy products are rapidly increasing (*Godfray et al.*, 2010). Furthermore, the regions where foods are produced and consumed are becoming more disconnected (*Fader et al.*, 2013). All of these are putting a detrimental pressure on global food security. Consequence management of future climate driven variables that negatively impact crops can be optimized (*Afshar and Najafi*, 2013) and improved if we gain knowledge about the past association between climate and crops. In this study we showed that the most important modes of persistent yield variabilities of maize, rice, sorghum and soybean, with high confidence, are well correlated with local climatic patterns. Maize croplands in Europe, south of Asia and North America, rice harvesting regions in Oceania and South America, sorghum croplands in North and South America, Caribbean, west and southeast of Asia and soybean croplands in North and South America, Oceania and Europe experienced local climate variability to a large extent. Our results indicate that many large-scale climatic patterns and climatic oscillations have a statistically detectable influence on different modes of crop yield variability, even where these effects have been less studied, for example TSA, SAM and QBO. Largescale climate, especially the ones that are attributed to the Central Pacific Ocean and Atlantic Ocean are strongly correlated with many PCs. In the first three PCs of the crops, ENSO and NAO were found to be the most dominant climate oscillation patterns. While country scale crop yields datasets are coarse, this analysis provides insights for understanding the crop yield variability and joint dependencies between countries.

There are some limitations to the analysis presented here. The spatial coverage of the croplands used in this study is based on the croplands coverage in the year 2000

(*Portmann et al.*, 2010). Since the croplands coverage has been changing through time with different intensities, the spatial coverage of croplands (Figure 3 and Figure 4) and impacted areas (Table 2, Figure 4, Figure 5 and Figure 6 ) presented in this study might not reflect the exact coverage and impacted areas, especially in some countries with substantial cropland changes such as Brazil. In addition, we used country based yield data (*FAO*, 2016). Since this data set integrates the yield of rain fed and irrigated crops, the impact of climate on rain fed and irrigated crops were not separated. Technological advances, seeds improvement, using fertilizers, farming practices, political issues, social strife and civil unrest, strategies applied for food security at regional scales, climate, regional shortages of energy and water all impact crop productivity. In this study, we focused only on climate and more studies are required to unveil and separate the impacts of these factors.

Climatic drivers of crop yield variability provide a useful source for prediction purposes as forecasting systems are gradually becoming more skilled (*Mazrooei et al.*, 2015) in long-range prediction of certain global drivers of climate such as ENSO, NAO, SAM or PDO. For instance, the NOAA Earth System Research Laboratory produces statistical forecasts to predict the PDO (*Alexander et al.*, 2008), the predictability of this pattern alongside the PCs that are well correlated with PDO as well as identified SLC found here can be used for food security purposes in the nations whose crop yields were impacted by this pattern. Our findings in this research have important practical implications as identified co-varying countries, especially import-dependent ones could take advantage of the favorable impacts of the climatic pattern. In other words, the negative impacts of climate on crop yields in some countries can be modified by its positive impacts in other countries. When importdependent countries be informed about the potential nations to trade with, the devastating consequences could get relieved in case of emergency and the global food security can be improved tremendously. It would be important to confirm and gain a better

understanding of these results by conducting similar studies on a regional scale using more detailed local data. Understanding the impact of different aspects of climate on crops is essential in order to inform decision making for food security purposes. Policymakers need scientific information to develop effective management and adaptation interventions such as infrastructure, technology and insurance measurements to protect vulnerable populations and to ensure global food security. This project tried to enhance the knowledge of global food security field, which is of relevance to policy initiatives, decision makers, water and energy managers, government and non-government organizations like United States Department of Agriculture (USDA) and Food and Agricultural Organization of United Nations (FAO), stakeholders and scientists with similar interests to ours. In the future, we will investigate more staple crops such as wheat and barley using the same methodology. In addition, the characteristics of the sparse matrix resulting from RPCA, particularly its association with climate, will be explored.

**Acknowledgments**

This study was supported and monitored by National Oceanic and Atmospheric Administration (NOAA) under Grant CUNY-CREST Cooperative agreement # NA16SEC4810008. The statements contained within the research article are not the opinions of the funding agency or the U.S. government, but reflect the authors opinions.

**Author contributions**

E.N., I.P. and R.K. designed the research. E.N. performed analyses, discussed the results, and wrote the manuscript. E.N. and I.P. contributed to respond to reviewers.

**Conflict of interest**

None of the authors has competing/conflicting interests in relation to the issues tackled in this paper.

**References**

Abdolrahimi, M. (2016), The effect of el niÃśo southern oscillation (enso) on world cereal production, *University of Sydney, Faculty of Agriculture and Environment*, *66*.

Afshar, A., and E. Najafi (2013), Consequence management of chemical intrusion in water distribution networks under inexact scenarios, *Journal of Hydroinformatics*, *16*(1), 178, doi:10.2166/hydro.2013.125.

Alexander, M. A., L. Matrosova, C. Penland, J. D. Scott, and P. Chang (2008), Forecasting pacific ssts: Linear inverse model predictions of the pdo, *Journal of Climate*, *21*(2), 385– 402, doi:10.1175/2007JCLI1849.1.

Armal, S., and R. Al-Suhili (2019), An urban flood inundation model based on cellular automata, *International Journal of Water*.

Armal, S., N. Devineni, and R. Khanbilvardi (2018), Trends in extreme rainfall frequency in the contiguous united states: Attribution to climate change and climate variability modes, *Journal of Climate*, *31*(1), 369–385.

Asadieh, B., N. Y. Krakauer, and B. M. Fekete (2016), Historical trends in mean and extreme runoff and streamflow based on observations and climate models, *Water*, *8*(5), doi:
10.3390/w8050189.

Baldwin, M. P., L. J. Gray, T. J. Dunkerton, K. Hamilton, P. H. Haynes, W. J. Randel, J. R. Holton, M. J. Alexander, I. Hirota, T. Horinouchi, D. B. A. Jones, J. S. Kinnersley, C. Marquardt, K. Sato, and M. Takahashi (2001), The quasi-biennial oscillation, *Reviews of Geophysics*, *39*(2), 179–229, doi:10.1029/1999RG000073.

Camberlin, P., S. Janicot, and I. Poccard (2001), Seasonality and atmospheric dynamics of the teleconnection between african rainfall and

tropical sea-surface temperature: Atlantic vs. enso, *International Journal of Climatology*, *21*(8), 973–1005, doi:10.1002/joc.673.

Candes, E. J., X. Li, Y. Ma, and J. Wright (2009), Robust principal component analysis?, *CoRR*, *abs/0912.3599*.

Chen, C., B. McCar, and C. Chang (2008), Strong el niño-southern oscillation events and the economics of the international rice market, *Climate Research*, *36*(2), 113–122, doi:
10.3354/cr00738.

Chen, C.-C., B. A. McCarl, and D. E. Schimmelpfennig (2004), Yield variability as influenced by climate: A statistical investigation, *Climatic Change*, *66*(1), 239–261, doi:
10.1023/B:CLIM.0000043159.33816.e5.

Chunzai, W., and E. D. B. (), The tropical western hemisphere warm pool, *Geophysical Research Letters*, *28*(8), 1635–1638, doi:10.1029/2000GL011763.

d Amour, C. B., L. Wenz, M. Kalkuhl, J. C. Steckel, and F. Creutzig (2016), Teleconnected food supply shocks, *Environmental Research Letters*, *11*(3), 035,007.

Dado, J. M. B., and H. G. Takahashi (2017), Potential impact of sea surface temperature on rainfall over the western philippines, *Progress in Earth and Planetary Science*, *4*(1), 23, doi:10.1186/s40645-017-0137-6.

Dai, A., K. E. Trenberth, and T. Qian (2004a), A global dataset of palmer drought severity index for 1870–2002: relationship with soil moisture and effects of surface warming, *Journal of Hydrometeorology*, *5*(6), 1117–1130.

Dai, A., K. E. Trenberth, and T. Qian (2004b), A global dataset of palmer drought severity index for 1870âĂŞ2002: Relationship with soil moisture

and effects of surface warming, *Journal of Hydrometeorology*, *5*(6), 1117–1130, doi:10.1175/JHM-386.1.

Demsar, U., P. Harris, C. Brunsdon, A. F. Stewart, and S. McLoone (2013), Principal component analysis on spatial data: An overview, *Annals of the Association of American Geographers*, *103*(1), 106–128, doi:10.1080/00045608.2012.689236.

Enfield, D. B., A. M. Mestas-NuÃśez, D. A. Mayer, and L. Cid-Serrano (1999), How ubiquitous is the dipole relationship in tropical atlantic sea surface temperatures?, *Journal of Geophysical Research: Oceans*, *104*(C4), 7841–7848, doi:10.1029/1998JC900109.

Enfield, D. B., A. M. Mestas-NuÃśez, and P. J. Trimble (2001), The atlantic multidecadal oscillation and its relation to rainfall and river flows in the continental u.s., *Geophysical Research Letters*, *28*(10), 2077–2080, doi:10.1029/2000GL012745.

Engelbrecht, C. J., and W. A. Landman (2016), Interannual variability of seasonal rainfall over the cape south coast of south africa and synoptic type association, *Climate Dynamics*, *47*(1), 295–313, doi:10.1007/s00382-015-2836-2.

Fader, M., D. Gerten, M. Krause, W. Lucht, and W. Cramer (2013), Spatial decoupling of agricultural production and consumption: quantifying dependences of countries on food imports due to domestic land and water constraints, *Environmental Research Letters*, *8*(1), 014,046.

FAO (2016), Food and agriculture organization of the united nations, http://www.fao.org/faostat/en/#data.

Friedman, M., and A. Schwartz (1991), Alternative approaches to analyzing economic data, *American Economic Review*, *81*(1), 39–49.

Garnett, E. R., M. L. Khandekar, and J. C. Babb (1998), On the utility of enso and pna indices for long-lead forecasting of summer weather over the crop-growing region of the canadian prairies, *Theoretical and Applied Climatology*, *60*(1), 37–45, doi:10.1007/ s007040050032.

Gershunov, A., and T. P. Barnett (1998), Interdecadal modulation of enso teleconnections, *Bulletin of the American Meteorological Society*, *79*(12), 2715–2726, doi:10.1175/ 1520-0477(1998)079<2715:IMOET>2.0.CO;2.

Gimeno, L., P. Ribera, R. Iglesias, L. d. l. Torre, R. GarcÃ?Â?a, and E. HernÃ?Â¡ndez (2002), Identification of empirical relationships between indices of enso and nao and agricultural yields in spain, *Climate Research*, *21*(2), 165–172, doi:10.3354/cr021165. Godfray, H. C. J., J. R. Beddington, I. R. Crute, L. Haddad, D. Lawrence, J. F. Muir, J. Pretty, S. Robinson, S. M. Thomas, and C. Toulmin (2010), Food security: The challenge of feeding 9 billion people, *Science*, *327*(5967), 812–818, doi:10.1126/science.

1185383.

Gonsamo, A., J. M. Chen, and D. Lombardozzi (), Global vegetation productivity response to climatic oscillations during the satellite era, *Global Change Biology*, *22*(10), 3414– 3426, doi:10.1111/gcb.13258.

Gouveia, C., R. M. Trigo, C. C. DaCamara, R. Libonati, and J. M. C. Pereira (2008), The north atlantic oscillation and european vegetation dynamics, *International Journal of Climatology*, *28*(14), 1835–1847, doi:10.1002/joc.1682.

Guiling, W., and Y. Liangzhi (2004), Delayed impact of the north atlantic oscillation on biosphere productivity in asia, *Geophysical Research Letters*.

Handler, P. (1984), Corn yields in the united states and sea surface temperature anomalies in the equatorial pacific ocean during the period 1868âĂŞ1982, *Agricultural and Forest Meteorology*, *31*(1), 25 – 32, doi:https://doi.org/10.1016/0168-1923(84)90003-0.

Hansen, J. W., A. W. Hodges, and J. W. Jones (1998), Enso influences on agriculture in the southeastern united states, *Journal of Climate*, *11*(3), 404–411, doi:10.1175/ 1520-0442(1998)011<0404:EIOAIT>2.0.CO;2.

Heino, M., M. J. Puma, P. J. Ward, D. Gerten, V. Heck, S. Siebert, and M. Kummu (2018), Two-thirds of global cropland area impacted by climate oscillations, *Nature Communications*, *9*(1), 1257, doi:10.1038/s41467-017-02071-5.

Heisey, P. W. (2015), Crop yields and global food security: Will yield increase continue to feed the world?, *American Journal of Agricultural Economics*, *97*(2), 661–663, doi:10.

1093/ajae/aau121.

Henley, B. J., J. Gergis, D. J. Karoly, S. Power, J. Kennedy, and C. K. Folland (2015), A tripole index for the interdecadal pacific oscillation, *Climate Dynamics*, *45*(11), 3077– 3090, doi:10.1007/s00382-015-2525-1.

Hirst, A. C., and S. Hastenrath (1983), Diagnostics of hydrometeorological anomalies in the zaire (congo) basin, *Quarterly Journal of the Royal Meteorological Society*, *109*(462), 881–892, doi:10.1002/qj.49710946213.

Iizumi, T., J.-J. Luo, A. J. Challinor, G. Sakurai, M. Yokozawa, H. Sakuma, M. E. Brown, and T. Yamagata (2014a), Impacts of el niño southern oscillation on the global yields of major crops, *Nature Communications*, *5*, 3712 EP –, article.

Iizumi, T., J.-J. Luo, A. J. Challinor, G. Sakurai, M. Yokozawa, H. Sakuma, M. E. Brown, and T. Yamagata (2014b), Impacts of el niño southern oscillation on the global yields of major crops, *Nature communications*, *5*, 3712.

Jolliffe, I. T. (2002), *Principal Component Analysis, Second Edition*, Springer-Verlag New York.

Jury, M. R. (2002), Economic impacts of climate variability in south africa and development of resource prediction models, *Journal of Applied Meteorology*, *41*(1), 46–55, doi:

10.1175/1520-0450(2002)041<0046:EIOCVI>2.0.CO;2.

Kerr, R. A. (2000), A north atlantic climate pacemaker for the centuries, *Science*, *288*(5473), 1984–1985, doi:10.1126/science.288.5473.1984.

Kim, M.-K., and B. A. McCarl (2005), The agricultural value of information on the north atlantic oscillation: Yield and economic effects, *Climatic Change*, *71*(1), 117–139, doi:

10.1007/s10584-005-5928-x.

Knight, J. R., C. K. Folland, and A. A. Scaife (2006), Climate impacts of the atlantic multidecadal oscillation, *Geophysical Research Letters*, *33*(17), doi:10.1029/2006GL026242.

Krishnan, R., and M. Sugi (2003), Pacific decadal oscillation and variability of the indian summer monsoon rainfall, *Climate Dynamics*, *21*(3), 233–242, doi:10.1007/ s00382-003-0330-8.

Leathers, D. J., B. Yarnal, and M. A. Palecki (1991), The pacific/north american teleconnection pattern and united states climate. part i: Regional temperature and precipitation associations, *Journal of Climate*, *4*(5), 517–528, doi:10.1175/1520-0442(1991)004<0517:

TPATPA>2.0.CO;2.

Legler, D. M., K. J. Bryant, and J. J. O'Brien (1999), Impact of enso-related climate anomalies on crop yields in the u.s., *Climatic Change*, *42*(2), 351–375, doi:10.1023/A:

1005401101129.

Li, Y., W. Ye, M. Wang, and X. Yan (2009), Climate change and drought: a risk assessment of crop-yield impacts, *Climate research*, *39*(1), 31–46.

Linkin, M. E., and S. Nigam (2008a), The north pacific oscillationâĂŞwest pacific teleconnection pattern: Mature-phase structure and winter impacts, *Journal of Climate*, *21*(9), 1979–1997, doi:10.1175/2007JCLI2048.1.

Linkin, M. E., and S. Nigam (2008b), The north pacific oscillationâĂŞwest pacific teleconnection pattern: Mature-phase structure and winter impacts, *Journal of Climate*, *21*(9), 1979–1997, doi:10.1175/2007JCLI2048.1.

Lobell, D. B., and C. B. Field (2007), Global scale climate–crop yield relationships and the impacts of recent warming, *Environmental research letters*, *2*(1), 014,002.

Lobell, D. B., W. Schlenker, and J. Costa-Roberts (2011), Climate trends and global crop production since 1980, *Science*, *333*(6042), 616–620, doi:10.1126/science.1204531.

Malone, R., D. Meek, J. Hatfield, M. Mann, R. Jaquis, and L. Ma (2009), Quasi-biennial corn yield cycles in iowa, *Agricultural and Forest Meteorology*, *149*(6), 1087 – 1094, doi: https://doi.org/10.1016/j.agrformet.2009.01.009.

Mantua, N. J., and S. R. Hare (2002), The pacific decadal oscillation, *Journal of Oceanography*, *58*(1), 35–44, doi:10.1023/A:1015820616384.

Marshall, G. J. (2003), Trends in the southern annular mode from observations and reanalyses, *Journal of Climate*, *16*(24), 4134–4143, doi:10.1175/1520-0442(2003)016<4134:

TITSAM>2.0.CO;2.

Mazrooei, A., T. Sinha, A. Sankarasubramanian, S. Kumar, and C. D. Peters-Lidard (2015), Decomposition of sources of errors in seasonal streamflow forecasting over the u.s. sunbelt, *Journal of Geophysical Research: Atmospheres*, *120*(23), 11,809–11,825, doi:

10.1002/2015JD023687.

Mourtzinis, S., B. V. Ortiz, and D. Damianidis (2016), Climate change and enso effects on southeastern us climate patterns and maize yield, *Scientific Reports*, *6*, 29,777 EP –, arti-

cle.

Najafi, E., N. Devineni, R. M. Khanbilvardi, and K. Felix (2018a), Understanding the changes in global crop yields through changes in climate and technology, *Earth's Future*,

*6*(3), 410–427, doi:10.1002/2017EF000690.

Najafi, E., I. Pal, and R. Khnbilvardi (2018b), Diagnosing extreme drought characteristics across the globe, *Science and Technology Infusion Climate Bulletin,42nd NOAA Annual Climate Diagnostics and Prediction Workshop*, doi:doi:10.7289/V5/ CDPW-NWS-42nd-2018.

Nan, S., and J. Li (2003), The relationship between the summer precipitation in the yangtze river valley and the boreal spring southern hemisphere annular mode, *Geophysical Research Letters*, *30*(24), doi:10.1029/2003GL018381.

Nicholson, S. E., and D. Entekhabi (1987), Rainfall variability in equatorial and southern africa: Relationships with sea surface temperatures along the southwestern coast of africa, *Journal of Climate and Applied Meteorology*, *26*(5), 561–578, doi:10.1175/ 1520-0450(1987)026<0561:RVIEAS>2.0.CO;2.

NOAA-ESRL (2017), Noaa earth system research laboratory,http://www.esrl.noaa.gov/psd/.

ORNL (2016), Spatial data access tool (sdat). ornl daac, oak ridge, tennessee, usa. https://doi.org/10.3334/ornldaac/1388.

Osborne, T. M., and T. R. Wheeler (2013), Evidence for a climate signal in trends of global crop yield variability over the past 50 years, *Environmental Research Letters*, *8*(2), 024,001.

Penland, C., and L. Matrosova (1998), Prediction of tropical atlantic sea surface temperatures using linear inverse modeling, *Journal of Climate*, *11*(3), 483–496, doi:10.1175/ 1520-0442(1998)011<0483:POTASS>2.0.CO;2.

Podesta, G. P., C. D. Messina, M. O. Grondona, and G. O. Magrin (1999), Associations between grain crop yields in central-eastern argentina and el niÃ±oâĂŞsouthern oscillation, *Journal of Applied Meteorology*, *38*(10), 1488–1498, doi:10.1175/1520-0450(1999) 038<1488:ABGCYI>2.0.CO;2.

Porkka, M., M. Kummu, S. Siebert, and O. Varis (2013), From food insufficiency towards trade dependency: A historical analysis of global food availability, *PLOS ONE*, *8*(12), 1–12, doi:10.1371/journal.pone.0082714.

Portmann, F. T., S. Siebert, and P. DÃűll (2010), Mirca2000âĂŤglobal monthly irrigated and rainfed crop areas around the year 2000: A new high-

resolution data set for agricultural and hydrological modeling, *Global Biogeochemical Cycles*, *24*(1), n/a–n/a, doi:10.1029/ 2008GB003435, gB1011.

Poshtiri, M. P., and I. Pal (2016), Patterns of hydrological drought indicators in major u.s. river basins, *Climatic Change*, *134*(4), 549–563, doi:10.1007/s10584-015-1542-8.

Pournasiri Poshtiri, M., and I. Pal (2014), Variability of low flow magnitudes in the upper colorado river basin: identifying trends and relative role of large-scale climate dynamics, *Hydrology and Earth System Sciences Discussions*, *11*, 8779–8802, doi:10.5194/ hessd-11-8779-2014.

Power, S., F. Tseitkin, S. Torok, B. Lvery, R. Dahni, B. McAvaney, and S. Torok (1998), Australian temperature, australian rainfall and the southern oscillation, 1910-1992: coherent variability and recent changes, *australian meteorological magazine*, p. 47 (2): 85âĂŞ101, magazine.

Prabhu, A., J. Oh, I.-w. Kim, R. H. Kripalani, A. K. Mitra, and G. Pandithurai (2017), Summer monsoon rainfall variability over north east regions of india and its association with eurasian snow, atlantic sea surface temperature and arctic oscillation, *Climate Dynamics*, *49*(7), 2545–2556, doi:10.1007/s00382-016-3445-4.

Puma, M. J., S. Bose, S. Y. Chon, and B. I. Cook (2015), Assessing the evolving fragility of the global food system, *Environmental Research Letters*, *10*(2), 024,007.

Ray, D. K., J. S. Gerber, G. K. MacDonald, and P. C. West (2015), Climate variation explains a third of global crop yield variability, *Nature communications*, *6*.

Rogers, J. C., and R. V. Rohli (1991), Florida citrus freezes and polar anticyclones in the great plains, *Journal of Climate*, *4*(11), 1103–1113, doi:10.1175/1520-0442(1991)

004<1103:FCFAPA>2.0.CO;2.

Saji, N. H., and T. Yamagata (2003), Possible impacts of indian ocean dipole mode events on global climate, *Climate Research*, *25*(2), 151–169, doi:10.3354/cr025151.

Saji, N. H., B. N. Goswami, P. N. Vinayachandran, and T. Yamagata (1999), A dipole mode in the tropical indian ocean, *Nature*, *401*, 360 EP –.

Shi, X., J. Sun, D. Wu, L. Yi, and D. Wei (2015), Impact of autumn sst in the japan sea on winter rainfall and air temperature in northeast china, *Journal of Ocean University of China*, *14*(4), 604–611, doi:10.1007/s11802-015-2477-4.

Steffen, W., J. Sims, J. Walcott, and G. Laughlin (2011), Australian agriculture: coping with dangerous climate change, *Regional Environmental Change*, *11*(1), 205–214, doi:10.1007/ s10113-010-0178-5.

Steptoe, H., S. E. O. Jones, and H. Fox (2017), Correlations between extreme atmospheric hazards and global teleconnections: Implications for multihazard resilience, *Reviews of Geophysics*.

Tian, D., S. Asseng, C. J. Martinez, V. Misra, D. Cammarano, and B. V. Ortiz (2015), Does decadal climate variation influence wheat and maize production in the southeast usa?, *Agricultural and Forest Meteorology*, *204*, 1 – 9, doi:https://doi.org/10.1016/j.agrformet. 2015.01.013.

Trenberth, K. E., and J. W. Hurrell (1994), Decadal atmosphere-ocean variations in the pacific, *Climate Dynamics*, *9*(6), 303–319, doi:10.1007/BF00204745.

Trenberth, K. E., and D. P. Stepaniak (2001), Indices of el niÃśo evolution, *Journal of Climate*, *14*(8), 1697–1701, doi:10.1175/1520-0442(2001)014<1697:LIOENO>2.0.CO;2.

Troy, T. J., C. Kipgen, and I. Pal (2015), The impact of climate extremes and irrigation on us crop yields, *Environmental Research Letters*, *10*(5), 054,013.

Wallace, J. M., and D. S. Gutzler (1981), Teleconnections in the geopotential height field during the northern hemisphere winter, *Monthly Weather Review*, *109*(4), 784–812, doi: 10.1175/1520-0493(1981)109<0784:TITGHF>2.0.CO;2.

Wang, C., and B. Enfield, David (2003a), A further study of the tropical western hemisphere warm pool, *Journal of Climate*, *16*(10), 1476–1493, doi:10.1175/1520-0442(2003) 016<1476:AFSOTT>2.0.CO;2.

Wang, C., and D. B. Enfield (2003b), A further study of the tropical western hemisphere warm pool, *Journal of Climate*, *16*(10), 1476–1493, doi:10.1175/1520-0442-16.10.1476.

Wolter, K., and M. S. Timlin (2011), El niÃśo/southern oscillation behaviour since 1871 as diagnosed in an extended multivariate enso index (mei.ext), *International Journal of Climatology*, *31*(7), 1074–1087, doi:10.1002/joc.2336.

Yuan, C., and T. Yamagata (2015), Impacts of iod, enso and enso modoki on the australian winter wheat yields in recent decades, *Scientific Reports*, *5*, 17,252 EP –, article.

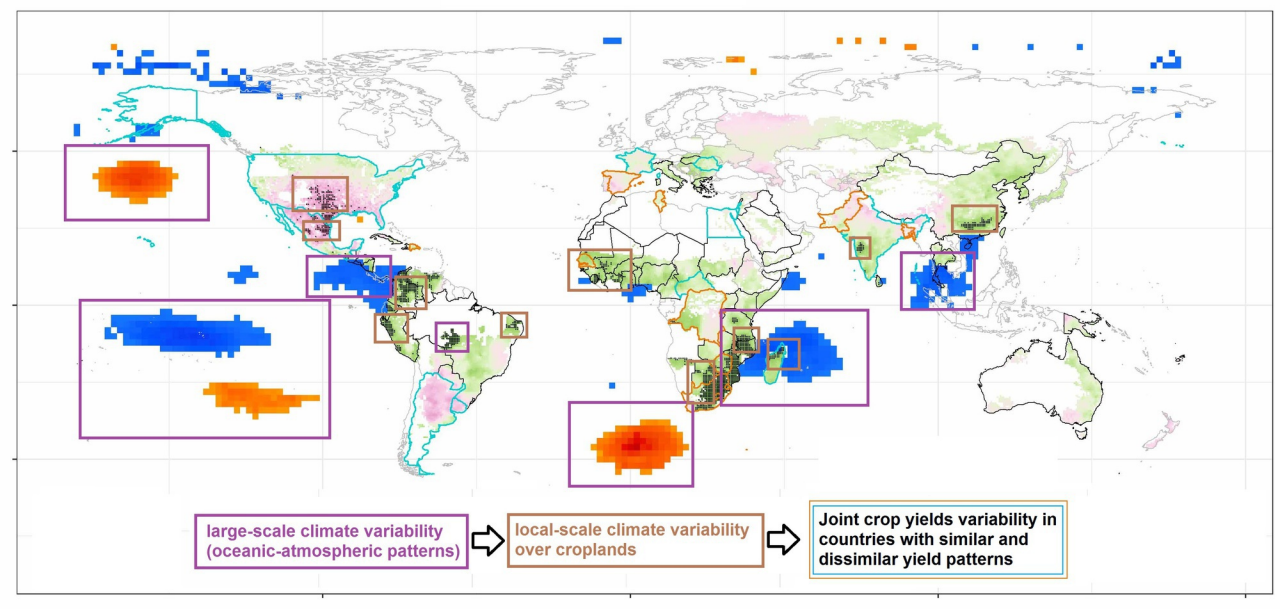
large-scale climate variability (oceanic-atmospheric patterns)
local-scale climate variability over croplands
Joint crop yields variability in countries with similar and dissimilar yield patterns